Theoretical Analysis of the Adsorption of Late Transition-Metal Atoms on the (001) Surface of Early Transition-Metal Carbides

Tatiana Gómez,[†,‡] Elizabeth Florez,[†,§] José A. Rodriguez,[||] and Francesc Illas*[,†]

Departament de Química Física & Institut de Química Teòrica i Computacional (IQTCUB), Universitat de Barcelona, C/ Martí i Franquès 1, 08028 Barcelona, Spain, Departamento de Química, Facultad de Ecología y Recursos Naturales, Universidad Andrés Bello, Republica 275, Santiago, Chile, Departamento de Física, Universidad de Chile, Las Palmeras 3425, Ñuñoa, Santiago, Chile, and Chemistry Department, Brookhaven National Laboratory, Upton, New York 11973

Received: October 27, 2009; Revised Manuscript Received: December 3, 2009

The interaction of atoms of Groups 9, 10, and 11 with the (001) surface of TiC, ZrC, VC, and δ-MoC has been studied by means of periodic density functional calculations using slab models. The calculated values of the adsorption energy are rather large, especially for Groups 9 and 10 elements ($E_{ads} = 3-6$ eV), but without clear trends along the series. Nevertheless, the analysis of the interaction at different sites indicates that the adsorbed atoms will be relatively mobile. Many of the admetals are electronically perturbed upon interaction with the carbide surfaces. Co, Ni, Cu, and Rh adatoms get positively or negatively charged, depending on the nature of the carbide substrate. Ir, Pd, Pt, and Au adatoms are always negatively charged. An analysis of the Bader charges for the most stable sites provides strong evidence that the most negative charge on the adatoms corresponds to the interaction with ZrC, followed by TiC. In the case of VC and δ-MoC, the charge on the adsorbed atoms may be slightly positive and of the same order for both carbides. The effect of the underlying carbide is large, with ZrC and TiC being predicted as the supports with the largest effect on the electronic structure of the adsorbed atoms with direct implications for the use of these systems in catalysis.

I. Introduction

Motivated by the excellent catalytic properties of early transition-metal carbides toward many chemical reactions[1−3] and by the discovery of the unexpected reactivity of Au nanoparticles supported on various oxides,[4−7] Rodriguez et al.[8] have investigated the electronic properties and reactivity of model systems involving small Au clusters supported on a well-defined TiC(001) substrate. The electronic structure of these systems was analyzed using synchrotron-based photoemission, regular X-ray photoelectron spectroscopy (XPS), and periodic density functional calculations. It was found that the presence of the underlying carbide induced a strong electron polarization on the supported Au particles. This could strongly affect their chemical activity with obvious implications for catalysis. In fact, new model catalysts based on Au nanoparticles supported on TiC(001) have been prepared, characterized, and experimentally tested toward SO_2 and thiophene dissociation and the reaction mechanism analyzed by means of density functional calculations.[9,10] In both cases, the catalytic activity and chemical performance of the Au/TiC system appear to be better than that of similar systems, such as Au/TiO_2 or Au/MgO.

The unexpected role of the TiC support on the catalytic activity of Au nanoparticles leads to an important new family of Au supported catalysts[9−11] and, at the same time, raises several questions. For instance, one may wonder whether other transition-metal carbides have similar or better performance or whether other transition-metal atoms or particles will show unexpected chemistry when supported on these carbides. In a recent work, we have analyzed, in detail, the adsorption and diffusion of Au atoms on a series of transition-metal carbides and found that the adsorption energy is sufficiently large to allow for Au migration through the surface before desorption can occur and that, indeed, migration is facilitated by rather low energy barriers.[12] Following this research, Florez et al. investigated the effect of the transition-metal carbide on the polarization of the supported Au nanoparticle electron density for a series of Au nanoparticles from Au_2 to Au_{14} and found that TiC and ZrC are the substrates inducing a larger polarization and, hence, the best candidates to be tested as catalytic systems.[13]

Expanding this research line and as a previous step before considering supported nanoparticles from metals other than Au, here, we present a systematic study of the adsorption of various transition-metal atoms (Co, Rh, Ir, Ni, Pd, Pt, Cu, Ag, and Au) on the (001) surface of VC, ZrC, TiC, and δ-MoC. The mail goal of the present study is to unravel possible trends in the interaction of these transition-metal atoms with the carbide surface, focusing essentially on the variation of the adsorption energy along the series for each one of the transition-metal carbides studied in the present work and on the net charge on the adatom. The latter can be used as a measure of the capability of the underlying substrate to polarize a given type of transition-metal atom, thus providing valuable information about possible metal/carbide couples to be tested in catalytic experiments.

II. Computational Details and Surface Models

The interaction of transition-metal atoms (Co, Rh, Ir, Ni, Pd, Pt, Cu, Ag, and Au) with the VC(001), TiC(001), ZrC(001),

* To whom correspondence should be addressed. E-mail: francesc.illas@ub.edu. Phone: +34934021229. Fax: +34934021231.
[†] Universitat de Barcelona.
[‡] Universidad Andrés Bello.
[§] Universidad de Chile.
[||] Brookhaven National Laboratory.

10.1021/jp910273z
Published on Web 12/23/2009

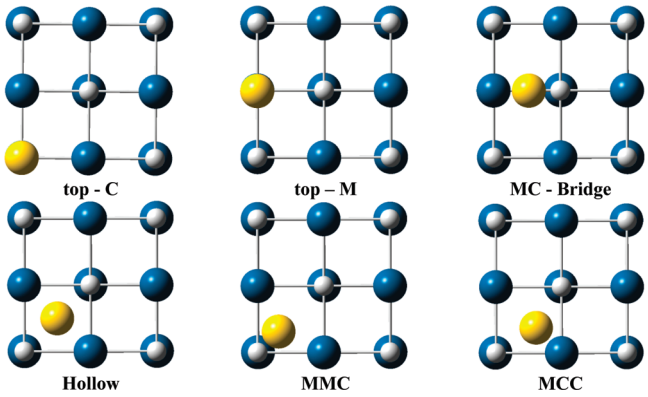

Figure 1. Different initial adsorption sites for transition-metal atoms (Co, Rh, Ir, Ni, Pd, Pt, Cu, Ag, and Au) on the (001) of transition-metal carbides. Small white, large blue, and large yellow spheres represent C, metal, and transition-metal atoms, respectively.

and δ-MoC(001) has been studied by means of calculations based on density functional theory (DFT), within the usual Kohn−Sham formalism, carried out for suitable periodic representations of these surfaces. The PW91 form of the generalized gradient approximation (GGA) has been chosen for the exchange-correlation potential.[14] The effect of the atomic cores on the valence electron density has been taken into account by means of the projected augmented plane-wave (PAW) method of Blöchl,[15] as implemented by Kresse and Joubert[16] in the VASP code.[17,18] This representation of the core states allows one to obtain converged results with a cutoff kinetic energy of 415 eV for the plane-wave basis set. The Monkhorst−Pack scheme[19] has been used to select the special *k*-points used to carry out the numerical integrations in the reciprocal space. A conjugated gradient algorithm with an energy criterion of 0.001 eV has been used for the atomic convergence, ensured forces to be, in all cases, smaller than 0.03 eV/Å. Spin-polarization calculations were carried out to obtain the energies of the isolated atoms and for several systems, including the transition-metal atom above the slab surface model. However, for the latter systems, the calculations converged always to a solution without or with negligible spin polarization. Note that this is contrary to the case of transition-metal atoms on the MgO(001) surface where the adatoms tend to maintain the electronic configuration of the isolated atoms.[20,21] This is a first indication that the interaction of transition-metal atoms with transition-metal carbides (TMCs) is significantly different from the interaction with simple oxides, such as MgO. In the forthcoming discussion, we will come back to this point.

The corresponding TMC (001) surfaces have been modeled by slab models repeated periodically with a vacuum region of 10 Å between repeated slabs. The slabs are constructed using the lattice parameter optimized for the bulk and reported in previous work.[22] They contain four atomic layers, and the two outermost ones of one side of the slab are completely allowed to relax. Transition-metal atoms of the Co, Rh, Ir, Ni, Pd, Pt, Cu, Ag, and Au series were placed above the (001) surface of TMCs, starting from six different possible adsorption sites (Figure 1). These are on top of a carbon atom (top-C), on top of a metal atom (top-M), bridging two metals and one carbon atom (MC-bridge), above the center of a square (Hollow), bridging two metals and one carbon atom (MMC), and bridging one metal and two carbon atoms (MCC). The calculations were carried out for a coverage of 0.25 metal monolayers with respect to the total number of M and C atoms in a carbide surface using a $(\sqrt{2} \times \sqrt{2})$ R45° unit cell.

Once the final geometries were obtained, a proper vibrational analysis has been used to characterize final geometries as minimum energy structures or as transition states (TS) and the corresponding adsorption energies calculated as

$$E_{ads} = -\{E_{TM/TMC} - (E_{TM} + E_{TMC})\}$$

where E_{TM} is the spin-polarized energy of the isolated metal atom (Co, Rh, Ir, Ni, Pd, Pt, Cu, Pt, or Au), E_{TMC} is the total energy of the relaxed surface, and $E_{TM/TMC}$ is the energy of the TMC (001) surface with the absorbed metal atoms. Here, it is worth pointing out that the energy of the isolated atoms corresponds to a d^8s^1 for Co, Rh, and Ir; d^9s^1 for Ni, Pd, and Pt; and $d^{10}s^1$ for Cu, Ag, and Au. Note that, in some cases, this is not the experimental ground state of the isolated atoms because of the inherent difficulty of DFT to describe atomic multiplets, as already pointed out by Bagus and Bennett[23] and Zieglet et al.[24] for SCF-Xα calculations and later by Baerends et al.[25] for LDA and GGA calculations dealing with the lowest electronic configurations of transition-metal atoms.[20,21]

To better understand the nature of the interaction of the different metals with the TMC surfaces, the net atomic charges in the preferred adsorption sites have been obtained from a topological analysis of charge density, which allows one to define atomic charges in a rigorous way.[26]

III. Results and Discussion

A. Adsorption Sites and Adsorption Energies. Figure 1 shows the different adsorption sites considered in the present study. We have investigated the adsorption of the metal atoms on a top (C or M), bridge, and hollow (standard four-fold Hollow, MMC, and MCC) sites. The interaction of Co, Rh, Ir, Ni, Pd, Pt, Cu, Ag, and Au on the TiC(001), Zr(001), VC(001), and δ-MoC(001) surfaces exhibits a rich landscape, as shown by the summary of results presented in Figures 2−4, collecting the calculated value of the adsorption energy for the most stable site. We have grouped the metals according to their group in the periodic table. Overall, the adsorption energy is large, ranging from 3 to almost 6 eV for Co, Rh, and Ir on the different substrates, followed by the Ni, Pd, and Pt group with energies in almost the same range but with noticeably smaller values, and, finally, by the Cu, Ag, and Au group with significantly smaller values in the 1.5−2.5 eV range, approximately. The large value of the adsorption energy is in agreement with the closed-shell nature of the electronic ground state. Here, at variance of what has been reported for transition-metal atoms on MgO(001),[21] the analysis of the density of states (not shown) shows that the interaction is strong enough to create a large gap between bonding and antibonding states with a concomitant filling of the former ones, resulting in a closed-shell electronic structure. Interestingly enough, the effect of the substrate is only moderate because, for a given metal atom, the difference between the largest and smallest adsorption energy values is at most 0.5 eV.

The strong nature of the interaction contrasts with the relatively flat character of the corresponding potential energy surface, evidenced by the appearance of nearly degenerate structures. Except for the case of the ZrC(001) surface, each transition-metal atom seems to differ in the preference of a special site or to exhibit multiple sites with similar energy. In the case of ZrC(001), all the transition-metal atoms considered in the present work prefer to sit at the top-C sites. However, for the TiC(001) surface, where one expects a similar behavior,

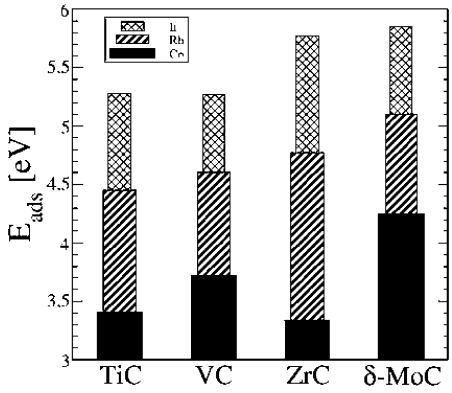

Figure 2. Adsorption energy (E_{ads} in eV) for Co, Rh, and Ir at the most stable site (see text) of the TiC(001), VC(001), ZrC(001), and δ-MoC(001) surfaces.

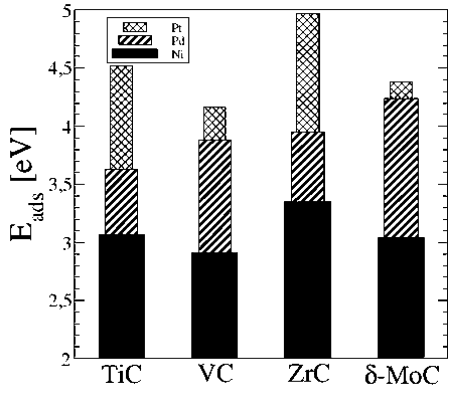

Figure 3. Adsorption energy (E_{ads} in eV) for Ni, Pd, and Pt at the most stable site (see text) of the TiC(001), VC(001), ZrC(001), and δ-MoC(001) surfaces.

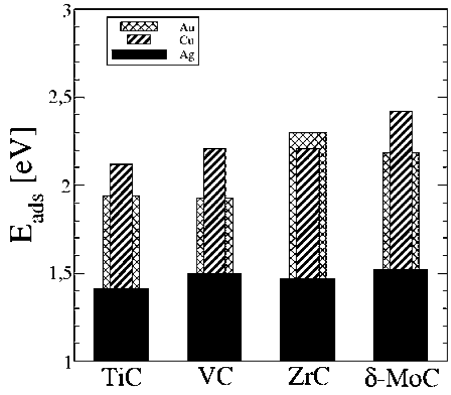

Figure 4. Adsorption energy (E_{ads} in eV) for Cu, Ag, and Au at the most stable site (see text) of the TiC(001), VC(001), ZrC(001), and δ-MoC(001) surfaces.

Co prefers the hollow site, while for Rh top-C, Hollow and MMC exhibit values of the adsorption energy differing in less than 0.05 eV. A similar situation is found for Ir where top-C and Hollow are nearly degenerate. On this surface, Ni behaves as Rh and Pd as Ir, whereas Pt, Cu, Ag, and Au all prefer the top-C site with no evidence of other stable positions in the sense that, in these cases, geometry optimization always converges to the top-C site independently from the starting geometry; for the atoms mentioned above, the optimization procedure is unable to switch to another site, and indeed, for some of these sites, the total energy converged values differ for these different sites in 0.05 eV or less. This is a clear indication that, for these cases, the nature of the chemisorption bond is not directional and, as a consequence, the adsorbed atoms will be able to diffuse through the surface even at low temperature and that the diffusion path is likely to follow the line going from top-C to Hollow, passing through MMC sites. A similar situation is found for VC(001) where Co and Rh prefer to adsorb at the Hollow site, but Hollow and MMC are nearly degenerate for Ir. This is also the case for Ni, but for Pd and Pt, the top-C site becomes clearly preferred. For Cu, top-C and MMC are almost degenerate; Ag prefers top-C and Au MMC. Let us now briefly discuss the situation for δ-MoC(001). Here, Hollow is the most stable site for Co, Rh, and Ir, although, for the latter, the MMC site becomes degenerate. Ni prefers top-C, but for Pd, MMC, Hollow, MC-Bridge, and Top-C have all adsorption energies within 0.06 eV, whereas for Pt, MMC and Hollow are the near degenerate sites. Finally, Cu and Au prefer MMC, whereas this is degenerate to MC-bridge for Ag. To conclude, the analysis of the different adsorption sites shows that there are no general rules; in some cases, there is a clear preferred site that normally is either top-C or Hollow, whereas in some other cases, the potential energy surface is relatively flat despite the quite strong interaction. In the former cases, one expects the adatoms to be rather pinned to the surface, whereas in the latter, they are predicted to be rather mobile. It is important to remark that the proximity between the different adsorption sites and the small difference between the calculated adsorption energies at these sites will facilitate diffusion of these atoms through these TMC surfaces.

B. Calculated Charges for the Admetals. To shed some light on the rather diffuse trends discussed above for the adsorption energies, we have computed the Bader charge for each adsorbate on each transition-metal carbide at the most stable site. Here, it is worth to point out that, for the cases with sites with the nearly the same value of the adsorption energy, the calculated Bader charges may exhibit noticeable variations in the absolute value. However, the analysis of the Bader charges reveals some clear trends that will not be changed upon consideration of another nearly degenerate site. For instance, for all the metal atoms, the complete set of results summarized in Figures 5−7 provides compelling evidence that the charge transfer from the substrate to the adatom decreases in the ZrC > TiC > VC > δ-MoC sequence. Hence, a given transition-metal atom tends to become more negatively (or less positively) charged on ZrC than on TiC and more negatively charged on TiC than on VC. It is worth to point out that this trend has also been found recently for the interaction of small Au clusters on these transition-metal carbide surfaces.[13] Therefore, it appears that ZrC is the substrate leading to the strongest polarization of the adsorbed metallic species. Recently, it has been shown that the polarization of Au by TiC is at the origin of the very good performance of the Au/TiC system in the destruction or desulfurization of SO_2 and thiophene.[9,10] The present results provide further support to the recent claim that ZrC will be a better substrate.[13] On ZrC(001), Ir and Pt exhibit a larger negative charge than Au. Among the inexpensive metals (Co, Ni, and Cu), only the charge on cobalt is comparable to the charge on gold.

Next, let us analyze in some detail the trends for each metal group. For Co, Rh, and Ir, the net charge on the adatom follows the trend of adsorption energies in the sense that, for a given TMC, the atom with the largest value of the adsorption energy has also the more negative or less positive Bader charge. Note that this trend follows that of the corresponding electron affinity that increases along Group 9. For Group 10 elements, Figure 6 reveals a very similar trend: the Bader charge on the adatom

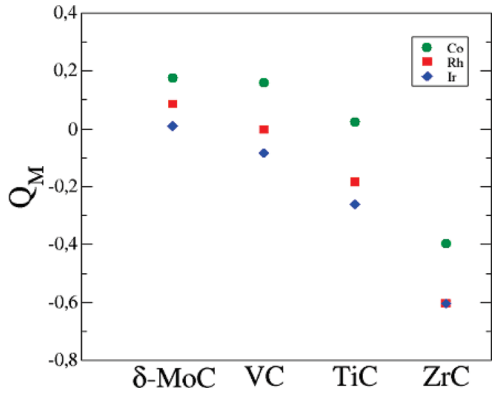

Figure 5. Calculated Bader charges (Q_M in au) for Co, Rh, and Ir at the most stable site (see text) of the TiC(001), VC(001), ZrC(001), and δ-MoC(001) surfaces.

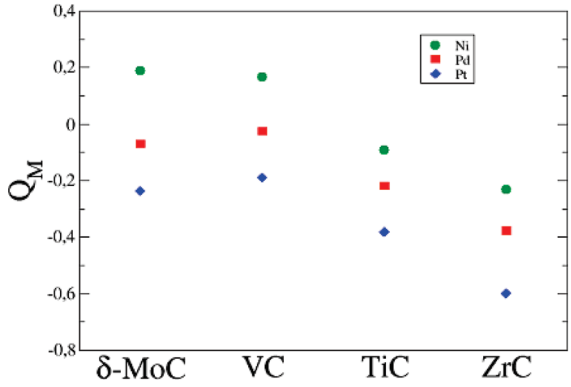

Figure 6. Calculated Bader charges (Q_M in au) for Ni, Pd, and Pt at the most stable site (see text) of the TiC(001), VC(001), ZrC(001), and δ-MoC(001) surfaces.

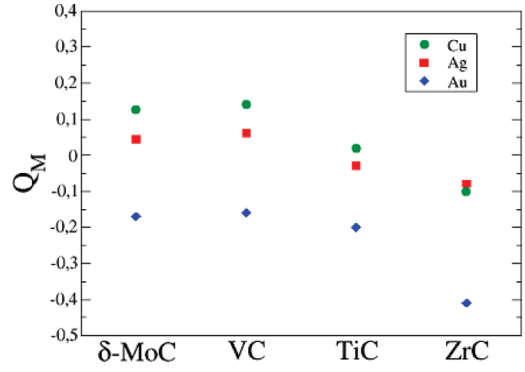

Figure 7. Calculated Bader charges (Q_M in au) for Cu, Ag, and Au at the most stable site (see text) of the TiC(001), VC(001), ZrC(001), and δ-MoC(001) surfaces.

follows the order of the calculated adsorption energy values for each TMC surface (Figure 3). Finally, Group 11 displays an intermediate behavior, where the largest degree of charge transfer corresponds to adsorbed Au (Figure 7), again, as expected from the electron affinity values, whereas, except for ZrC, Au tends to have adsorption energies intermediate between Cu and Ag. A more uniform trend is found when analyzing the Bader charges along the period. Thus, for all substrates, Co, Ni, and Cu are the adatoms with the smallest degree of charge transfer, leading either to the larger positive charges or to the smaller negative charges; see the top symbols in Figures 57. Following with this line of reasoning, we find that Rh, Pd, and Ag have intermediate charge and the corresponding calculated values appear in the intermediate zone of Figures 57. Lastly, Ir, Pt, and Au are the adatoms acquiring the most negative charge, which is consistent with the large electron affinity of these metal atoms.

IV. Conclusions

The interaction of atoms of Groups 9, 10, and 11 with the (001) surface of TiC, ZrC, VC, and δ-MoC has been studied by means of periodic density functional calculations and slab models. These calculations allowed us to predict the most stable sites and trends in the adsorption energy and to identify the important role of the underlying transition-metal carbide.

The calculated values of the adsorption energy are rather large, especially for Groups 9 and 10 elements, with values in the 3−6 eV range and noticeably smaller, but still significant, for Cu, Ag, and Au. An interesting feature of the resulting chemisorption bond is that, despite the large value of the adsorption energy, the potential energy surface around the most stable site appears to be relatively flat, indicating that, in most cases, the adatoms will easily diffuse at room temperature, thus also explaining their tendency to form larger particles. However, no clear trends or significant correlations are found between the calculated adsorption energy values and the type of carbide. Note, however, that the adsorption energy increases along a group except for Group 11.

The analysis of the Bader charges for the most stable sites provides strong evidence that the more negative charge on the adsorbed atom corresponds to the interaction with ZrC, followed by TiC. In the case of VC and δ-MoC, the charge on the adsorbed atom may be slightly positive and of the same order for both carbides. Thus, the present work supports recent findings indicating that Au/ZrC should outperform Au/TiC. In part, the trends exhibited by the calculated net charges on the adsorbed atoms follow the trend in electron affinity of the isolated atom. Ir and Pt exhibit a larger negative charge than Au, and among the inexpensive metals, only the charge on cobalt is comparable to the charge on gold.

To conclude, the interaction between transition-metal atoms and transition-metal carbides is rather strong, although the adsorbed species are predicted to be relatively mobile, and the effect of the underlying carbide is large, with ZrC and TiC being predicted as the supports with the largest effect on the electronic structure of the adsorbed atoms.

Acknowledgment. The authors wish to thank Dr. Francesc Viñes for carefully reading the manuscript and for useful comments. T.G. is grateful to the Universidad Andres Bello (Chile) for a Ph.D. fellowship and project UNAB-DI-02-9/I, and E.F. would like to thank Colciencias and the University of Antioquia (Colombia) for supporting her postdoctoral stay at the Universidad de Chile. Financial support has been provided by the Spanish MICINN (Grant FIS2008-02238), COST D-41 action, Generalitat de Catalunya (Grants 2009SGR1041 and XRQTC), and by Chile Fondecyt Grant 3080033. Computational time provided by the Barcelona Supercomputing Center (BSC) is gratefully acknowledged. The research carried out at Brookhaven National Laboratory was supported by the U.S. Department of Energy (Chemical Sciences Division, DE-AC02-98CH10886). The National Synchrotron Light Source (NSLS) is supported by the Divisions of Chemical and Materials Science of the U.S. Department of Energy.

Supporting Information Available: Table S1, containing numerical values for the adsorption energies plotted in Figures 24, and Table S2, containing numerical values for the Bader

charges plotted in Figures 57. This material is available free of charge via the Internet at http://pubs.acs.org.

References and Notes

(1) Levy, R. B.; Boudart, M. *Science* **1973**, *181*, 547.
(2) Oyama, S. T. *Catal. Today* **1992**, *15*, 179.
(3) Hwu, H. H.; Chen, J. G. *Chem. Rev.* **2005**, *105*, 185.
(4) (a) Haruta, M. *Catal. Today* **1997**, *36*, 153. (b) Haruta, M. *Nature* **2005**, *437*, 1098.
(5) Valden, M.; Lai, X.; Goodman, D. W. *Science* **1997**, *281*, 1647.
(6) Hashmi, A. S. K.; Hutchings, G. J. *Angew. Chem., Int. Ed.* **2006**, *45*, 7895.
(7) See also the reviews in the special issue dedicated to the chemistry of nano-gold in: *Chem. Soc. Rev.* **2008**, *37*.
(8) Rodriguez, J. A.; Viñes, F.; Illas, F.; Liu, P.; Takahashi, Y.; Nakamura, K. *J. Chem. Phys.* **2007**, *127*, 211102.
(9) Rodriguez, J. A.; Liu, P.; Viñes, F.; Illas, F.; Takahashi, Y.; Nakamura, K. *Angew. Chem., Int. Ed.* **2008**, *47*, 6685.
(10) Rodriguez, J. A.; Liu, P.; Takahashi, Y.; Nakamura, K.; Viñes, F.; Illas, F. *J. Am. Chem. Soc.* **2009**, *131*, 8595.
(11) Ono, L. K.; Roldán-Cuenya, B. *Catal. Lett.* **2007**, *113*, 86.
(12) Florez, E.; Viñes, F.; Rodriguez, J. A.; Illas, F. *J. Chem. Phys.* **2009**, *130*, 244706.
(13) Florez, E.; Feria, L.; Viñes, F.; Rodriguez, J. A.; Illas, F. *J. Phys. Chem. C* **2009**, *113*, 19994.
(14) Perdew, J.; Wang, Y. *Phys. Rev. B* **1992**, *45*, 13244.
(15) Bloch, E. *Phys. Rev. B* **1994**, *50*, 17953.
(16) Kresse, G.; Joubert, D. *Phys. Rev. B* **1999**, *59*, 1758.
(17) Kresse, G.; Hafner, J. *Phys. Rev. B* **1993**, *47*, 558.
(18) Kresse, G.; Furthmüller, J. *Phys. Rev. B* **1996**, *54*, 11169.
(19) Monkhorst, H. J.; Pack, J. D. *Phys. Rev. B* **1976**, *13*, 5188.
(20) López, N.; Paniagua, J. C.; Illas, F. *J. Chem. Phys.* **2002**, *117*, 9445.
(21) Markovits, A.; Paniagua, J. C.; López, N.; Minot, C.; Illas, F. *Phys. Rev. B* **2003**, *67*, 115417.
(22) Viñes, F.; Sousa, C.; Liu, P.; Rodriguez, J. A.; Illas, F. *J. Chem. Phys.* **2005**, *122*, 174709.
(23) Bagus, P. S.; Bennet, B. I. *Int. J. Quantum Chem.* **1975**, *9*, 143.
(24) Ziegler, T.; Rauk, A.; Baerends, E. J. *Theor. Chim. Acta* **1977**, *43*, 261.
(25) Baerends, E. J.; Branchadell, V.; Sodupe, M. *Chem. Phys. Lett.* **1997**, *265*, 481.
(26) Bader, R. F. W. *Atoms in Molecules: A Quantum Theory*; Oxford Science: Oxford, U.K., 1990.

JP910273Z